

Thermal and acid treatment of diatom frustules

E. Gulturk ^{a,*}, M. Guden ^b

^a Department of Mechanical Engineering, Cumhuriyet University, Sivas, Turkey

^b Department of Mechanical Engineering, Izmir Institute of Technology, Gulbahce Koyu, Urla, Izmir, Turkey

* Corresponding author: E-mail address: elifaras@cumhuriyet.edu.tr

Received 09.04.2011; published in revised form 01.06.2011

Manufacturing and processing

ABSTRACT

Purpose: Diatoms, belonging to Bacilariophyta family, are single-celled microscopic (1-100 micron) plants living in aquatic environment. The diatom cell is protected inside a shell (frustule) constructed from amorphous nano-silica particles. It is proposed that the frustules and purified silica powders obtained from frustules can be used to reinforce composites. In this study, microstructural properties of two diatom frustules were determined and different methods were investigated for silica powder processing from diatom frustules.

Design/methodology/approach: Natural (ND) and calcined (CD) diatom frustules were used in this study. The chemical and microscopic properties of the diatom frustules were determined using Scanning Electron Microscope (SEM), X-Ray Diffraction (XRD), Fourier Transform Infrared Spectrometry (FTIR) and energy dispersive X-Ray Florescence spectrometer (XRF). Two different processing routes were applied to process silica powder from diatom frustules. These included (i) leaching the frustules directly in HF, (ii) incorporating thermally treated frustules in to the liquid nitrogen.

Findings: At increasing HF concentrations, the variety of shapes, nanopores and open voids were seen on the surface of frustules as silica particles were removed from the surface. SEM micrograph results showed that HF significantly etched inside the existing pore structure of the diatom frustules. HF concentration was found more effective in mass loss than the leaching time. Thermal treatment induced several cracks propagated between macro pores and nanopores of the frustules.

Practical implications: Results show that thermal and acid treatments were not effective for obtaining silica powder from frustules. Ball milling can be used for silica powder processing from frustules in the further study.

Originality/value: In this paper, the microstructural properties of ND and CD frustules were determined. The effect of thermal and acid treatment on frustules was investigated with SEM.

Keywords: Diatom frustules; SEM; Acid leaching; Thermal treatment

Reference to this paper should be given in the following way:

E. Gulturk, M. Guden, Thermal and acid treatment of diatom frustules, Journal of Achievements in Materials and Manufacturing Engineering 46/2 (2011) 196-203.

1. Introduction

Diatoms are single-celled algae, belonging to the class of Bacilariophyceae of the phylum Bacilariophyta [1,2]. These are unicellular microscopic plants and inhabit all aquatic and moist

environments. The growth of diatoms is responsible for about 25% of the world primary food production. Each diatom cell develops an external cell wall known as frustules. The frustule is composite of amorphous silica and an organic material [2]. There are over 100 000 different species of diatoms classified by cell

wall geometry [1,2]. The dimensions of amorphous silica skeletons range from ~1-500 μm , while the regular features distributed on the frustules wall possess characteristic dimensions of 10-200 nm [3,4]. The diatom frustules are composed of two almost equal halves that fit together like a Petri dish, surrounding the bulk of the single cell within. The inner frustule is known as the hypotheca and the outer one as the epitheca. Each half (theca) consists of a valve which forms the larger outer surface and several ring-like silica structures known as girdle bands. Diatoms are classified in two major groups based on the frustules symmetry: pennate and centric [5]. Pennate types tend to be elongated and centric types of diatoms are radial symmetric [1]. When diatoms cells die and the remnant silica cell wall collect at the floor of the ocean, forming fossils. These fossilized cell walls are called diatomite or Diatomaceous Earth (DE) or Kieselguhr. DE is an abundant, extremely cheap material and extensively used in sound and heat insulation, chemical reactions as catalyst, sensor components, dynamites, pool water, beer and wine filtration, absorption and gel filtration [6,7,8,9]. The potential engineering and medical applications of diatom frustules have also recently been proposed, including metal film membranes, pinpoint drug delivery and processing of nano powder silica [2]. Diatomite frustules were also used as reinforcement elements in polymeric composites [10]. Frustules are primarily amorphous agglomerations of very small silica particles in the order of a few ten nanometers. Although silica crystals are very strong, the bonds between crystals in diatom frustules are presumed to be weaker than the intra-particle bonds. It was proposed that various techniques including high-energy ball milling, ultra-sonic waves and electric and thermal shock can break the relatively weak bonds between the diatom particles. The purified silica powders obtained from frustules can be used to reinforce composites [2].

In this study, we aimed to determine microstructural properties of frustules and receive silica powders from frustules. Two diatom frustules were characterized and the microstructures of both diatom frustules exposed to thermal shock, chemical treatment were investigated.

2. Materials for research

2.1. Characterization of diatom frustules

The first type of diatom frustules was a calcined diatomite (CD), obtained as diatomaceous earth filter material, Celatoms FW-60 grade (Eagle Picher Filtration & Mineral Inc, USA), received from a local vendor. The second was a natural diatomite (ND) received from Alfa Aesar, Johnson Matthey Co., England. The CD frustules were calcined above 1000°C for one hour by the producer. Initially, both frustules were dried in a laboratory oven at 120°C for 2 h. Following the drying, frustules were heat-treated for 2 h in a temperature range of 100 and 1200°C at the intervals of 100°C in order to assess the effect of the temperature on the crystal structure of frustules. The morphology of both diatom frustules was investigated using a XL-30S FEG Philips scanning electron microscope (SEM). X-Ray diffraction (XRD, X'Pert Pro, Philips, Holland) of the frustules was performed with Cu-K α

radiation ($\lambda=1.54 \text{ \AA}$) at 40kV in the 2θ intervals of 5-70°. The chemical composition of frustules was determined using an energy dispersive X-Ray Fluorescence spectrometer (XRF, Spectro IQ II). The chemical contents of frustules were determined by Fourier transform infrared spectroscopy, (FTIR, 8601 PC spectrometer, Shimadzu, Japan). FTIR analysis was performed in a range of wave number between 4000-400 cm^{-1} .

2.2. Silica powder processing from frustules

There different processing routes were applied to process silica powder from diatom frustules. These included (i) leaching the frustules directly in HF, (ii) incorporating thermally treated frustules in to the liquid nitrogen. The acid leaching was performed on ND and CD frustules at 1N hydrofluoric acid concentration for one hour to assess the effect of HF on frustules. Before leaching, ND frustules were heat treated at 600°C for 2 h. Amorphous ND and CD frustules were treated at different HF concentrations (1, 2, 3, 5, 7 and 9 N) for 7 days for distinct etching times (15 min, 30 min and 1, 24, 72, 120, 168 h). The solution containing frustules and HF was prepared as 1/10 frustules and HF ratio (g/mol). The solution was filtered and washed with deionized water to remove the ions and other residues. The resulting solid was finally dried at 110°C for 2 h and stored. The natural diatom frustules were heated to temperature in the range of 700-1200°C for about half an hour and then plunged into the liquid nitrogen for thermal treatment.

3. Results and discussion

3.1. Diatom frustules

Calcined frustules are observed under SEM (Figure 1(a)) and found mostly cylindrical in shape. The frustules appear as short tubes with the rows of fine pores, aligned parallel to the tube-axis (centric type). Figure 1(a) proves that the most of diatom frustules in CD belong to the genera *Melosira granulata*, with the short diameters of 5-20 μm . One of the ends of the frustules possesses a circular hole with a protruding outer rim, while the other end is closed with either a dense or porous layer and possesses finger-like protuberances as shown in Figure 1(a). The finger-like protuberances are observed to intercalate with other frustules forming paired chains of frustules [10]. The pore size of frustules is measured from the magnified SEM pictures and found to range between 200 and 600 nm. ND frustules mostly consist of pennate and centric types of diatoms as depicted in Figure 1(b). The pore diameter of ND frustules is measured to change between 200 and 1000 nm depending of the species of diatom frustules. It is also noted few of the frustules were broken probably during the milling applied by the producer.

The standardless XRF analysis results of CD and ND frustules are tabulated in Table 1. Both frustules are found to be composed of silica mineral (88-90%) and small amount of other oxide components. The higher Na content of CD frustule is mostly probably resulted from the flux addition in the calcination process.

Table 1
Chemical composition of the frustules.

Constituents	CD (wt%)	ND (wt%)
SiO ₂	88.16	90.08
Al ₂ O ₃	5.02	5.53
Fe ₂ O ₃	1.83	1.52
CaO	0.6	0.51
MgO	0.41	1.03
TiO ₂	0.19	0.21
Na ₂ O	2.78	<0.02
P ₂ O ₅	0.02	0.23
MnO	<0.002	<0.002
K ₂ O	0.031	0.48
Cr ₂ O ₃	0.084	0.089
Loss on ignition	1	

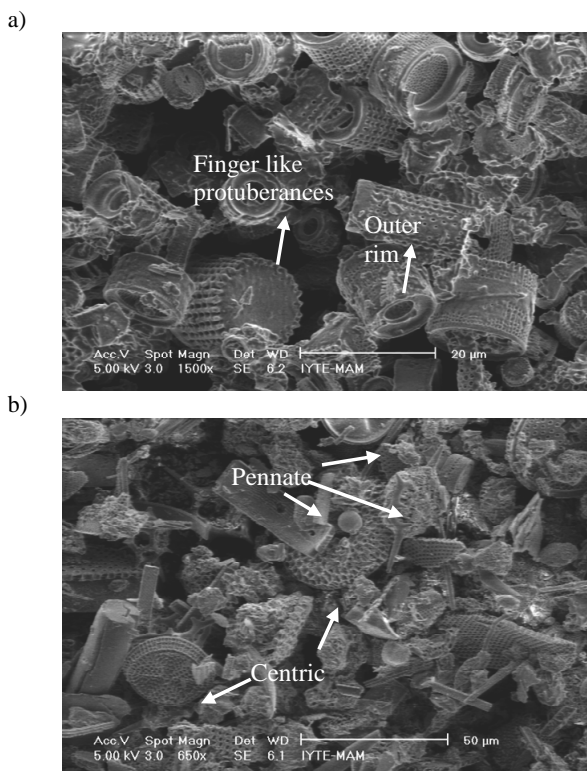


Fig. 1. SEM micrograph of diatomites, (a) CD frustules and (b) ND frustules.

XRD spectrum of the CD frustule is shown in Fig. 2. The structure is low crystalline cristobalite (SiO₂, Ref. 76-0940), which is tetragonal form of silica. X-Ray diffraction pattern of ND exhibits opal structure (SiO₂, Ref. 38-0448), which is hexagonal silica, with quartz (SiO₂, Ref. 82-0511) (Fig. 3). According to Yuan, et al. [11], Diatomaceous silica, the amorphous silica with Opal-A structure, exists in the form of frustule in the natural mineral assemblage of diatomite. X-ray diffraction pattern of ND further confirms that the frustules

consist of predominantly amorphous silica. CD structure represents the Opal C structure which is a well-ordered form of the silicate mainly in the α -cristobalite. The XRD spectra of the heat treated CD frustules between 100 and 1200°C show the same crystalline cristobalite silica peaks with those of as-received frustules. This confirms the stability of the as received CD frustules. The XRD patterns of as-received and heat treated ND are shown in Fig. 4. When the heat-treatment temperature of ND frustules increases to 900°C, the peak intensity of quartz at about $2\theta=26^\circ$ decreases and the transformation of amorphous phase into crystal structure starts (Fig. 4). The X-ray diffraction pattern of ND heat-treated at 1200°C exhibits crystalline cristobalite phase.

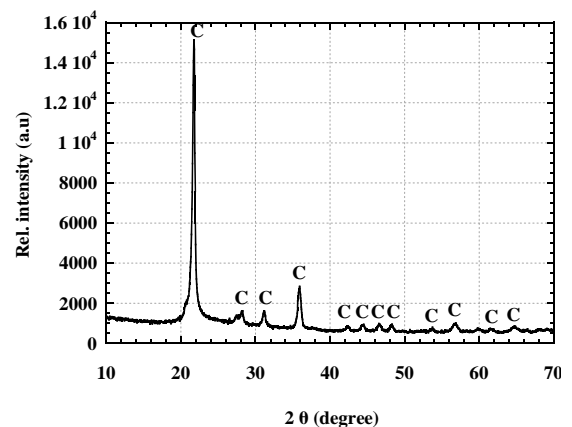


Fig. 2. XRD pattern of CD (C: Cristobalite, low)

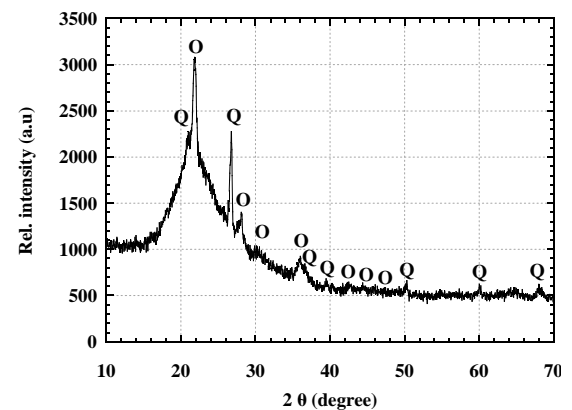


Fig. 3. XRD pattern of ND (Q: Quartz, O: Opal)

The FTIR charts of as-received CD and ND frustules are shown in Fig. 5. Both frustules show the same three characteristic broad bands at 1096, 797 and 471 cm⁻¹. The band detected at 1076-1100 cm⁻¹ is assigned to Si-O-Si anti-symmetric stretching mode. The adsorption band at 750-850 cm⁻¹ represents the symmetric Si-O-Si stretching mode. The wave numbers of 618 and 450 cm⁻¹ symbolize the bands characteristic of the Si-O-Si framework. There is one different peak at about 617 cm⁻¹ in CD frustules due to its crystal structure.

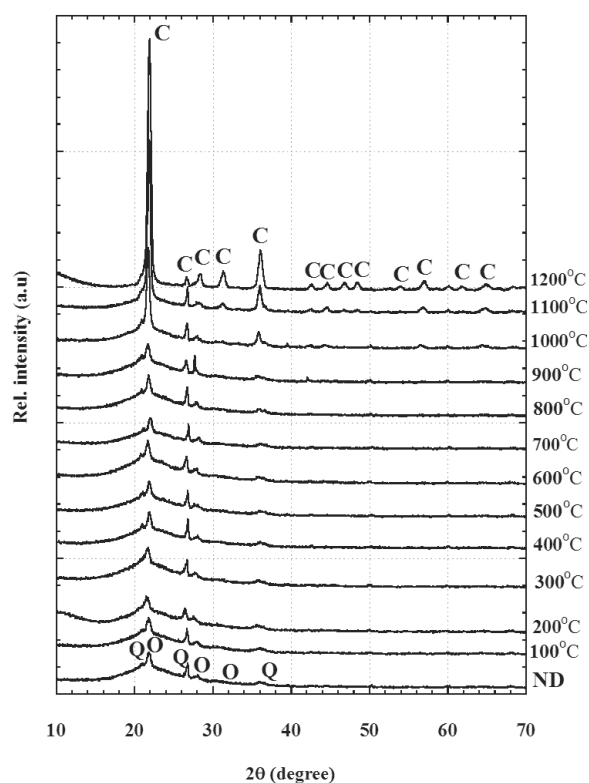


Fig. 4. XRD patterns of as-received and heat treated ND

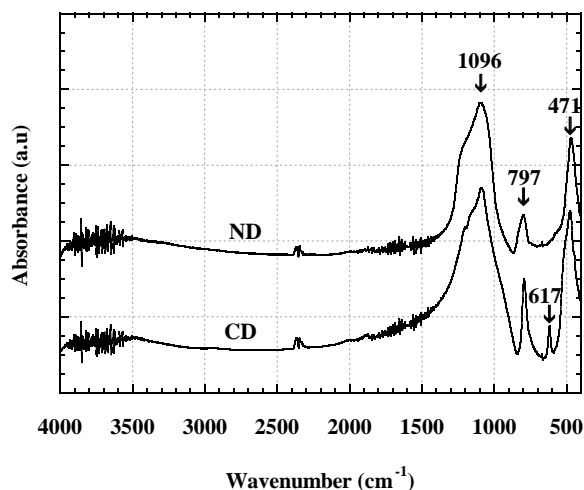


Fig. 5. FTIR charts of ND and CD frustules

The FTIR analysis of as-received and heat treated CD frustules show that there are no differences between the characteristic band of cristobalite phase from 400 to 1800 cm^{-1} . In the range from 400 to 1800 cm^{-1} , the spectra of as received and

treated ND samples show the same characteristic peaks at 1096, 797, and 471 cm^{-1} (Fig. 6), which are similar to amorphous silica. In addition to the above three bands, the spectrum of ND frustules treated at 1200 $^{\circ}\text{C}$ demonstrates a new band at 618 cm^{-1} , which indicates the transforms to cristobalite phase [12].

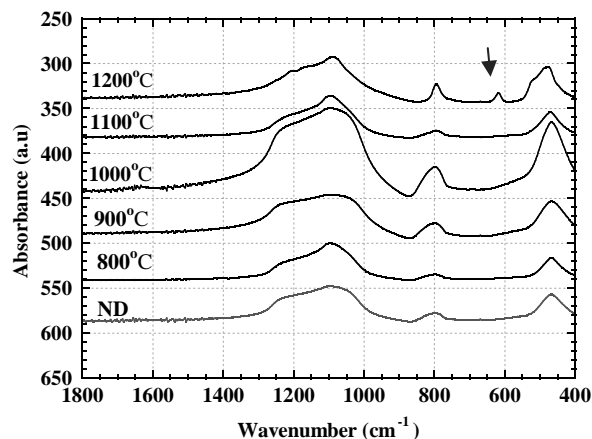


Fig. 6. FTIR analysis of as-received (red) and heat treated (black) ND frustules

3.2. Acid leaching

SEM micrographs of untreated CD frustules and treated frustules (1N and one hour leaching) are shown in Fig. 7. One hour acid leaching, as seen in Figures 7(b-d), result in destruction of frustule wall structure. Figures 7(c) and (d) show the surface structure of HF treated frustules at higher magnifications. The chemical treatment revealed the variety of rigid shapes and pores. The silica particles about 200-600 nm in size are clearly seen on the surface of frustules at higher magnifications. The dissolution of the frustule initially occurs between the grain boundaries.

Fig. 8(a) shows the ND frustules before acid leaching and Figures 8(a-d) after one hour HF leaching. As seen in Figures 8(a-d) acid leaching has less effect of the dissolution of the ND frustules than CD frustules. However, acid leaching is seen to increase the surface roughness of ND frustules by forming 10 nm to 100 nm pores on the surface (Fig. 8(d)). It is believed that the pores are formed as a result of dissolution and/or separation of the individual silica particles from the surface.

The SEM pictures of ND frustules exposed to different HF concentration for seven days are shown in Figures 9(a-d). ND frustules exhibit more rough and irregular surface structure with increasing HF concentration. At increasing HF concentrations a large attack on the exterior surface and interior pore wall are seen. HF significantly etches toward the inside the existing pore structure in diatom frustules due to their high content of silica. HF leaching effectively creates new pores and increases the pore properties. This phenomenon was also previously reported [13,14].

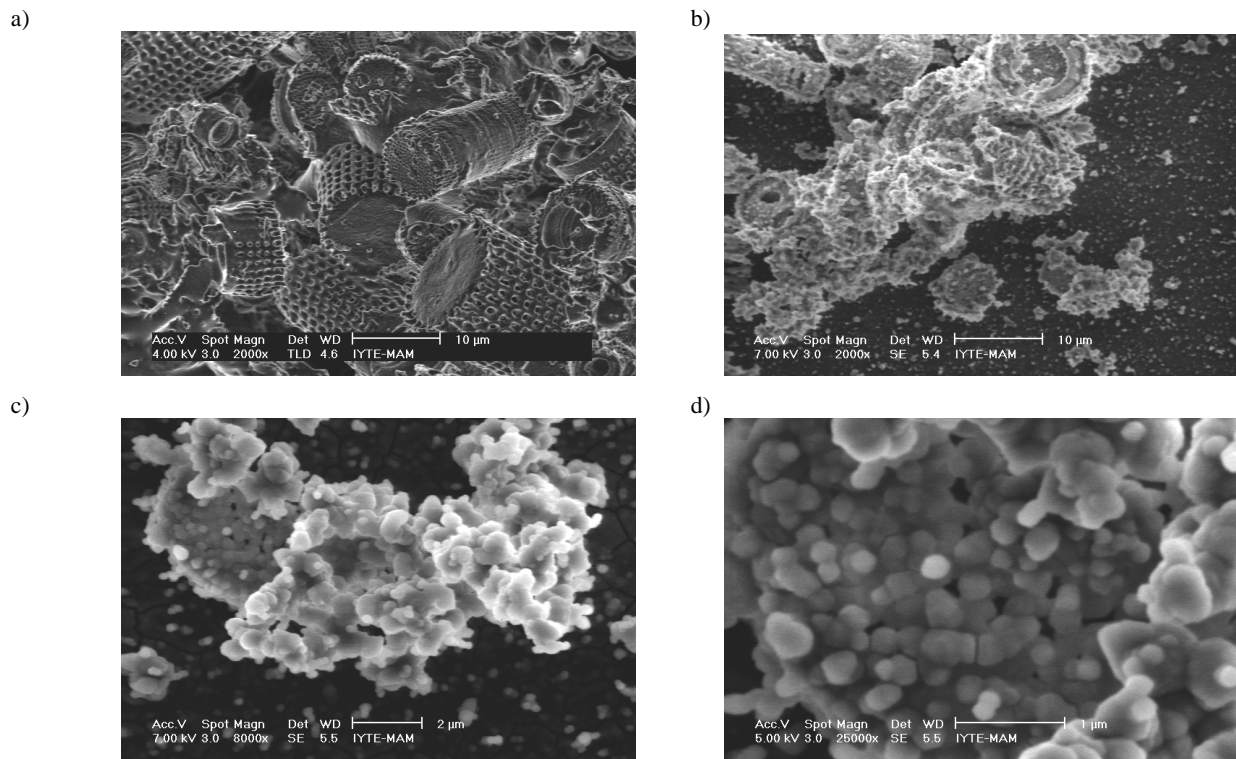


Fig. 7. SEM micrographs of CD frustules (a) before leaching, (b), (c) and (d) after 1N HF leaching for 1 hour

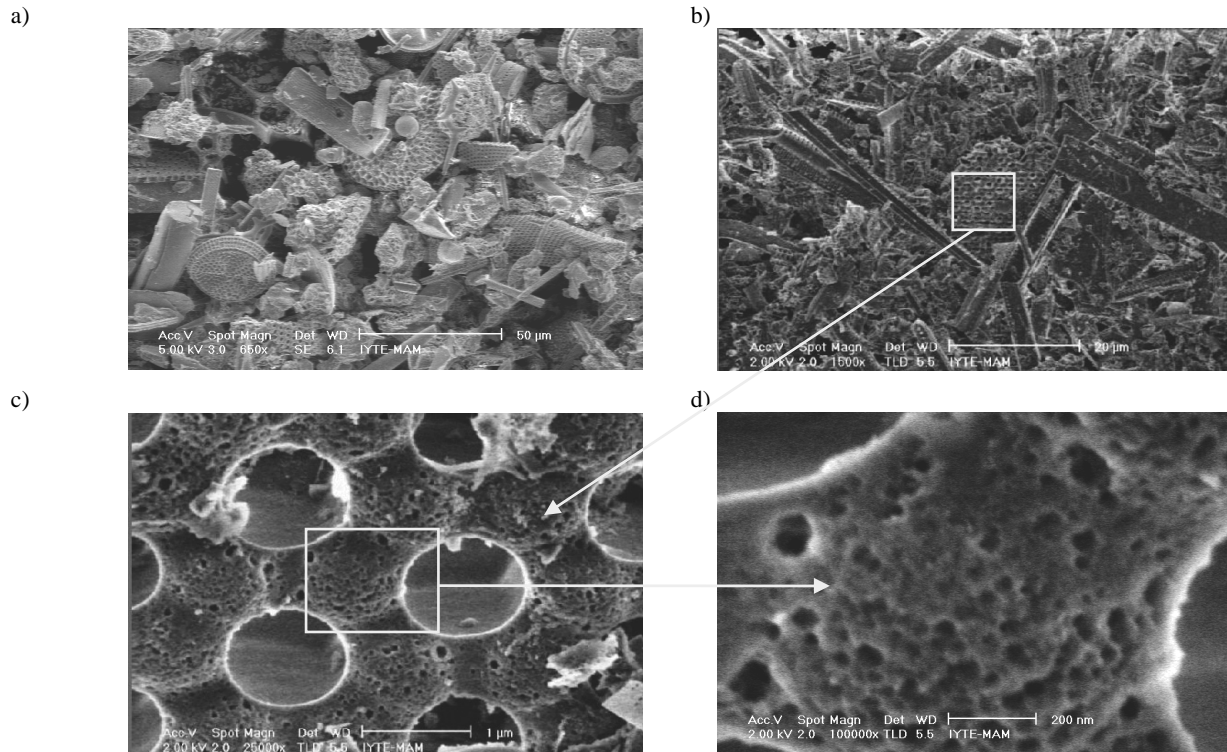


Fig. 8. SEM micrographs of CD frustules (a) before leaching, (b), (c) and (d) after 1N HF leaching for 1 hour

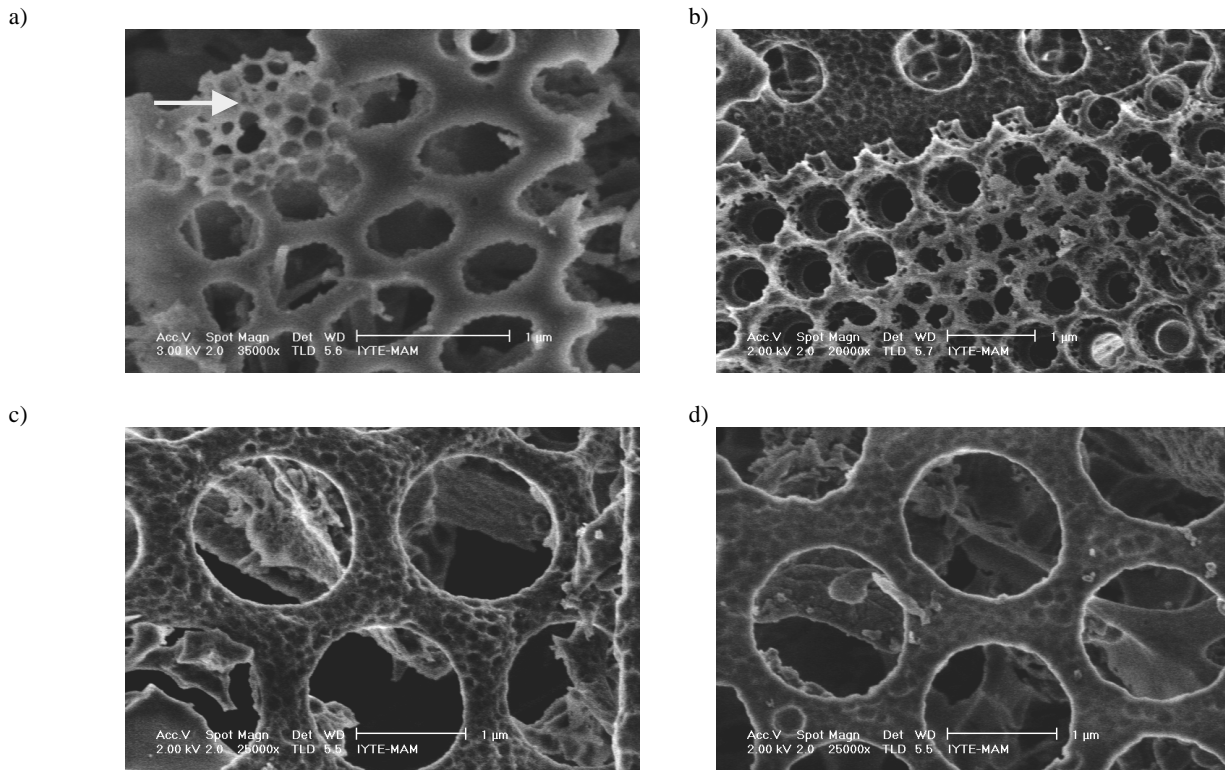


Fig. 9. SEM micrographs of ND frustules with treated (a) 1N, (b) 3N, (d) 5N, (e) 9N HF for 7 days

The mass loss of ND with HF concentration and leaching time are shown in Figures 10 and 11, respectively. While the mass loss is about 23% with increasing etching time, this value increases to 90% with increasing HF concentration. This observation shows a good agreement with the SEM observations as the surface area of modified frustules is rougher and larger. These results prove that HF concentration is more effective parameter to mass loss of ND frustules than leaching time.

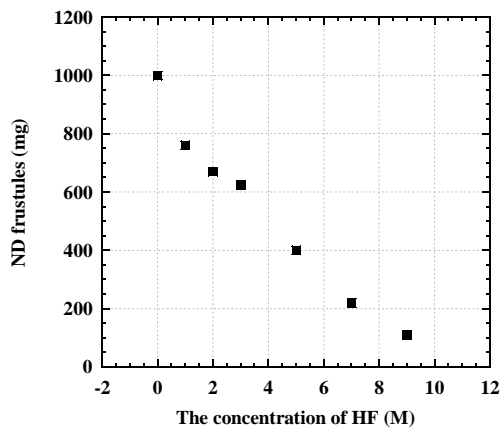


Fig. 10. The mass loss of ND at different HF concentration for 7 days

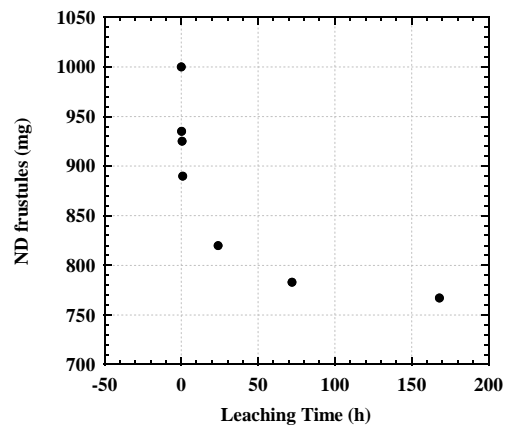


Fig. 11. The mass loss of ND at 1N HF for various leaching times

3.3. Thermal treatment

The numbers of cracks between the pores and broken frustules are generally seen in ND samples after the thermal shock (Figures 12(b) and (c)). The SEM micrographs of ND frustules quenched from 700°C show that the porous valve structure of frustules are more affected from the thermal shock than the girdle band structure (Figure 12 (c)).

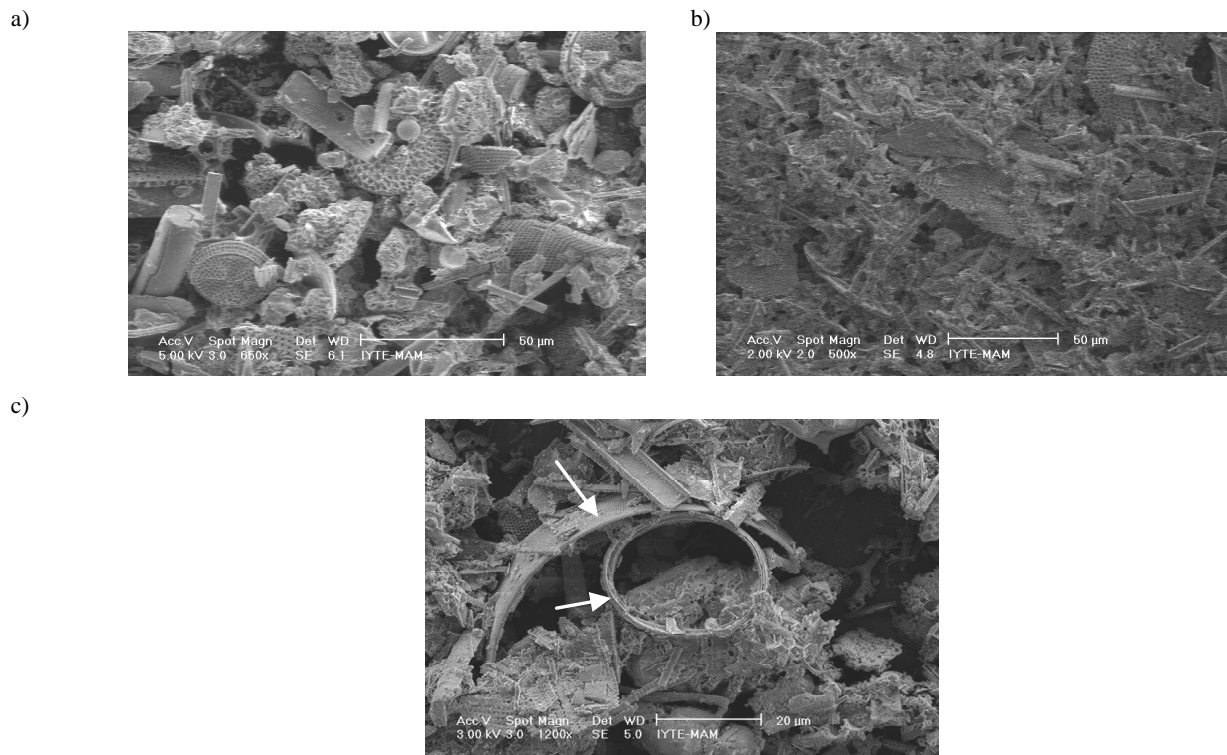


Fig. 12. SEM micrographs of CD frustules (a) before leaching, (b) and (c) after 1N HF leaching for 1hour

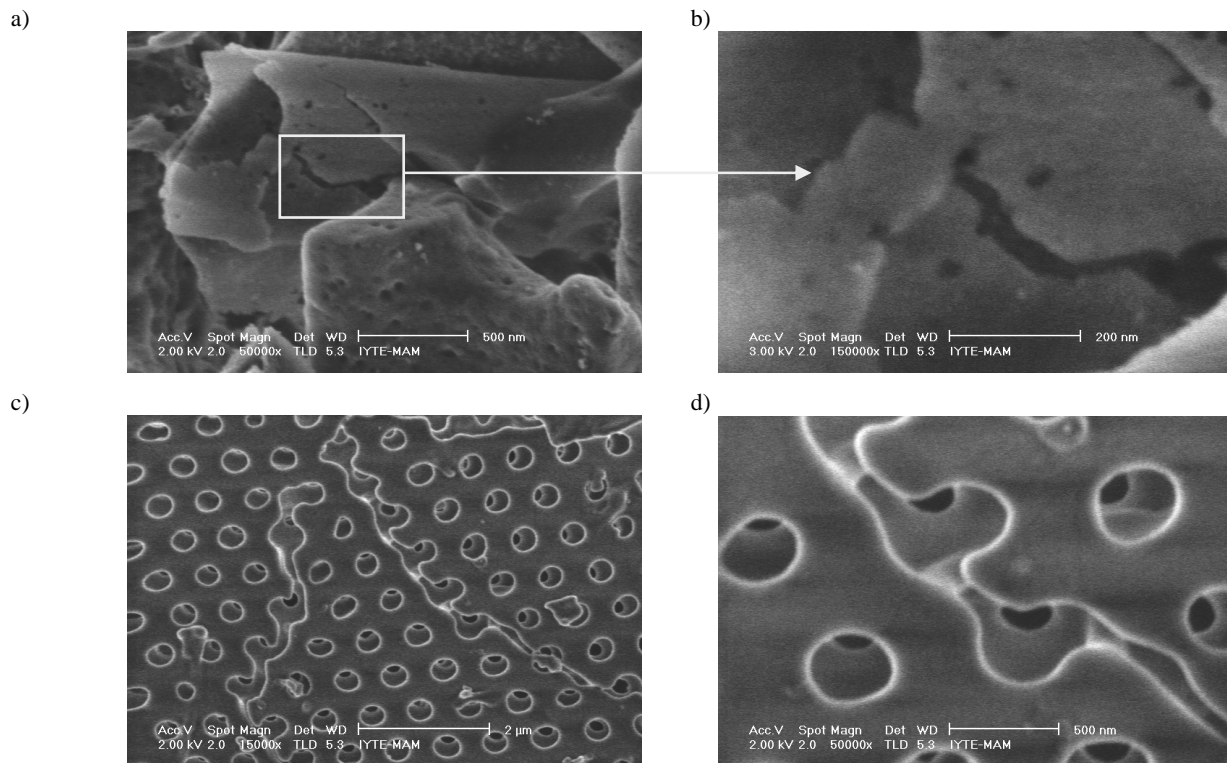


Fig. 13. The crack propagation in ND frustules quenched from (a), (b) 800°C, (c) and (d) 1200°C

The crack propagation is seen in Figures 13(a-d) for ND frustules quenched from 800°C and 1200°C. Despite the absence of plastic deformation and the smooth fracture surfaces of the broken frustules, the cracks are seen to propagate between nano pores as seen in Figures 13(a) and (b). This confirmed that the cracks travelled around the nano-silica spheres, ~40 nm, of the diatom frustules [15]. In ND frustules heated to 1200°C, the smoother surfaces of the fractured pieces are due to the transformation of the amorphous structure into cristobalite structure (Figures 13(c) and (d)).

4. Conclusions

The thermal treatment and acid leaching were performed to frustules to obtain silica powder from frustules. The acid leaching was applied to frustules at different concentrations and leaching times. At increasing HF concentrations, the variety of shapes, nanopores and open voids were seen on the surface of frustules as silica particles were removed from the surface. SEM micrograph results showed that HF significantly etched inside the existing pore structure of the diatom frustules. HF concentration was found more effective in mass loss than the leaching time. Thermal treatment induced several cracks propagated between macro pores and nanopores of the frustules. The observed smooth surfaces and grain boundaries of frustules at 1200°C was because of transformation of the amorphous structure into crystal phase. Finally, thermal treatment and acid leaching were no effective process for obtaining sub micron silica powders from natural frustules. In next study, the effect of ball milling process on frustules can be investigated for obtaining silica powders from frustules.

Acknowledgements

We acknowledge The Scientific and Technical Research Council of Turkiye (TUBITAK) for financial support to 106M186 project and İYTE-BAP for support to 2008İYTE04 project.

References

- [1] J. Parkinson, R. Gordon, Beyond micromachining: the potential of diatoms, *Trends in Biotechnology* 17 (1999) 190-196.
- [2] K.M. Wee, T.N. Rogers, B.S. Altan, S.A. Hackney, C. Hamm, Engineering and medical applications of diatoms, *Journal of Nanoscience and Nanotechnology* 5 (2005) 88-91.
- [3] T. Fuhrmann, S. Landwehr, M. El Rharbi-Kucki, M. Sumper, Diatoms as living photonic crystals, *Applied Physics B-Lasers and Optics* 78 (2004) 257-260.
- [4] C.S. Gaddis, K.H. Sandhage, Freestanding microscale 3D polymeric structures with biologically-derived shapes and nanoscale features, *Journal of Materials Research* 19 (2004) 2541-2545.
- [5] E.L. Goldberg, M.A. Grachev, V.A. Bobrov, A.V. Bessergenev, B.V. Zolotaryov, Y.V. Likhoshway, Do diatom algae frustules accumulate uranium? *Nuclear Instruments and Methods in Physics Research Section a-Accelerators Spectrometers Detectors and Associated Equipment* 405 (1998) 584-589.
- [6] Y. Cai, S.M. Allan, K.H. Sandhage, Three-dimensional magnesia-based nanocrystal assemblies via low-temperature magnesiothermic reaction of diatom microshells, *Journal of the American Ceramic Society* 88 (2005) 2005-2010.
- [7] S. Scala, C. Bowler, Molecular insights into the novel aspects of diatom biology, *Cellular and Molecular Life Sciences* 58 (2001) 1666-1673.
- [8] E.F. Stoermer, J.P. Smol, *The Diatoms: Applications for the Environmental and Earth Sciences*, Cambridge University Press, 2004.
- [9] J.E. Ongerth, P.E. Hutton, DE filtration to remove *Cryptosporidium*, *Journal of the American Water Works Association* 89 (1997) 39-4.
- [10] A. Tasdemirci, S. Yuksel, D. Karsu, E. Gulturk, I.W. Hall, M. Guden, Diatom frustule-filled epoxy: Experimental and numerical study of the quasi-static and high strain rate compression behaviour, *Materials Science and Engineering a-Structural Materials Properties Microstructure and Processing* 480 (2008) 373-382.
- [11] P. Yuan, H.P. He, D.Q. Wu, D.Q. Wang, L.J. Chen, Characterization of diatomaceous silica by Raman spectroscopy, *Spectrochimica Acta Part a-Molecular and Biomolecular Spectroscopy* 60 (2004) 2941-2945.
- [12] W.S. Xiao, W.S. Peng, G.X. Wang, F.Y. Wang, K.N. Weng, Infrared spectroscopic study of changbaishan diatomite, *Spectroscopy and Spectral Analysis* 24 (2004) 690-693.
- [13] W.T. Tsai, K.J. Hsien, and C.W. Lai, Chemical activation of spent diatomaceous earth by alkaline etching in the preparation of mesoporous adsorbents, *Industrial and Engineering Chemistry Research* 43 (2004) 7513-7520.
- [14] W.T. Tsai, C.W. Lai, K.J. Hsien, Characterization and adsorption properties of diatomaceous earth modified by hydrofluoric acid etching, *Journal of Colloid and Interface Science* 297 (2006) 749-754.
- [15] C.E. Hamm, R. Merkel, O. Springer, P. Jurkojc, C. Maier, K. Prechtel, V. Smetacek, Architecture and material properties of diatom shells provide effective mechanical protection, *Nature* 421 (2003) 841-843.